

Supporting Information

Effect of chain architecture on the swelling and thermal response of star-shaped thermo-responsive (poly(methoxy diethylene glycol acrylate)-*block*-polystyrene)₃ block copolymer films

Qi Zhong^{1,2,*}, *Lei Mi*¹, *Ezzeldin Metwalli*², *Lorenz Bießmann*², *Martine Philipp*²,
*Anna Miasnikova*³, *André Laschewsky*^{3,4}, *Christine M. Papadakis*², *Robert Cubitt*⁵,
*Matthias Schwartzkopf*⁶, *Stephan V. Roth*^{6,7}, *Jiping Wang*¹ and *Peter Müller-Buschbaum*^{2,*}

¹Key Laboratory of Advanced Textile Materials & Manufacturing Technology, Ministry of Education; Engineering Research Center for Eco-Dyeing & Finishing of Textiles, Ministry of Education; National Base for International Science and Technology Cooperation in Textiles and Consumer-Goods Chemistry, Zhejiang Sci-Tech University, 310018 Hangzhou, China

²Technische Universität München, Physik-Department, Lehrstuhl für Funktionelle Materialien/Fachgebiet Physik Weicher Materie, James-Franck-Str. 1, 85748 Garching, Germany

³Universität Potsdam, Institut für Chemie, Karl-Liebknecht-Str. 24-25, 14476 Potsdam-Golm, Germany

⁴Fraunhofer Institut für Angewandte Polymerforschung, Geiselbergstr. 69, 14476 Potsdam-Golm,
Germany

⁵Institut Laue-Langevin, 6 rue Jules Horowitz, 38000 Grenoble, France

⁶Deutsches Elektronen-Synchrotron (DESY), Photon Science, Notkestr. 85, 22607 Hamburg, Germany

⁷KTH Royal Institute of Technology, Department of Fibre and Polymer Technology, Teknikringen 56-
58, SE-100 44 Stockholm, Sweden

Synthesis of (PMDEGA-*b*-PS)₃

Azoisobutyronitrile (AIBN) was bought from Wako and crystallized twice from methanol. Styrene (purity 99%) was obtained from Sigma-Aldrich and purified by distillation prior to use. Deuterated water (D₂O) (purity 99.95%) was from Deutero GmbH. 1,4-Dioxane was obtained from Acros (purity 99.8%). Dichloromethane (purity 99.8%), aqueous ammonia solutions (NH₃, 30-33%) and hydrogen peroxide (H₂O₂, 30%) were received from Carl Roth GmbH. All organic solvents had a purity higher than 99 % and were used as received. Water used for the preparation of polymer solutions was purified by a Millipore Q Plus system, and when used, had pH=6 after equilibration in air. Monomer methoxy diethylene glycol acrylate MDEGA was prepared by titanium (IV) iso-propoxide catalyzed transesterification of ethyl acrylate with diethylene glycol monomethyl ether. The procedure as well as the synthesis of trifunctional chain transfer agent 1,1,1-*tris*(3-(4-(tert-butoxycarbonyl)-benzylsulfanylthiocarbonylsulfanyl)propanoyloxy) ethane (CTA) were described before.¹

For the synthesis of the star-shaped block copolymer (poly(methoxy diethylene glycol acrylate)-*block*-polystyrene)₃, denoted as (PMDEGA-*b*-PS)₃, a 3-arm star polystyrene trifunctional macroRAFT agent was prepared first. Styrene (3.40 g, 32.6 mmol) and CTA (0.644 g, 0.544 mmol) were purged with argon for 20 min, and heated at 110 °C for 18 h. The resulting yellow viscous liquid was diluted with acetone and precipitated thrice into methanol. The collected

polymer was dried in vacuo at ambient temperature for 1 d to give 1.87 g of yellow powder (yield 55 %; $M_n^{\text{theo}} = 3450 \text{ g mol}^{-1}$, $M_n^{\text{NMR}} = 3950 \text{ g mol}^{-1}$ by end group analysis, $M_n^{\text{app}} = 3800 \text{ g mol}^{-1}$ (SEC in THF, calibration by linear polystyrene standards), $\bar{D} = 1.15$). The terminal tert-butyl ester groups were then removed by stirring a 25 wt% solution of the star polystyrene in a 15:85 (w/w) mixture of dry trifluoroacetic acid and dichloromethane at 25 °C for 1 d. The solvent was removed under reduced pressure, the residue dissolved in benzene and lyophilized to yield the trifunctional macroRAFT agent as yellow powder ($M_n^{\text{NMR}} = 3800 \text{ g mol}^{-1}$, ratio R-groups/Z-groups = 1). In the final step, 5.46 g (31.4 mmol) of monomer MDEGA, 172 mg (0.048 mmol) of the macroRAFT agent, and 2.5 mg (0.015 mmol) of initiator azoisobutyronitrile in 19 ml of benzene were deoxygenated by bubbling argon for 20 min through the solution, and subsequently reacted at 70 °C for 5 h. Then, the reaction was quenched by immersing the flask into an ice bath. The star block copolymer was isolated and purified by thrice repeated precipitations into hexane. The yellowish gluey polymer was dried in vacuo for 3 d. Yield: quantitative; $M_n^{\text{theo}} = 115 \text{ kg mol}^{-1}$, $M_n^{\text{NMR}} = 117 \text{ kg mol}^{-1}$, $M_n^{\text{app}} = 41 \text{ kg mol}^{-1}$ (SEC in DMF, calibration by linear polystyrene standards), $\bar{D} = 1.8$.

Characterization of the polymers by ¹H NMR

¹H NMR spectra were taken with a Bruker Avance 300 (300 MHz) apparatus for chain transfer agents and monomers in CDCl₃, and for the polymers in acetone d₆. The ¹H NMR spectra of star polymer precursor (PS*)₃ with t-butyl ester end groups, the star polymer precursor (PS)₃ after removal of the t-butyl ester end groups, and the star block copolymer (PMDEGA-*b*-PS)₃ are displayed in Figure S1. The comparison of Figures S1a and S1b shows the disappearance of signal "u" and accordingly, the successful removal of the t-butyl groups by acid treatment.

From the spectra, the number average molar mass M_n of the polystyrene star macroCTA is determined via end-group analysis, by comparing the integral of the signal "t" at ca. 8.0 ppm (2 aryl CH at C-2 of the benzoic acid moieties) to the integral of the signal group "o, p, q+s" between 7.5 and 6.2 ppm (5 aryl CH of the styrene moieties, corrected for the value of 2 aryl CH at C-3 of the benzoic acid moieties).

$$M_n = M_r(CTA) + \{f \times DP_n^{arm} \times M_r(monomer)\} \quad (S1)$$

In which $M_r(CTA^*)=1183.67$ and $M_r(CTA)=1015.35$, $M_r(styrene)=104.15$, f (number of star arms) = 3, and

$$DP_n^{arm} = \{integral(o, p, q + s) - integral(s)\}/5 \quad (S2)$$

after normalization of the integrals to an intensity value equivalent of 6 protons for signal "t".

Combining equations S1 and S2, and knowing that $integral(s)=integral(t)$, we obtain from the integral values shown in Figure S1b for the polystyrene star (PS)₃ $M_n^{NMR}=3800$.

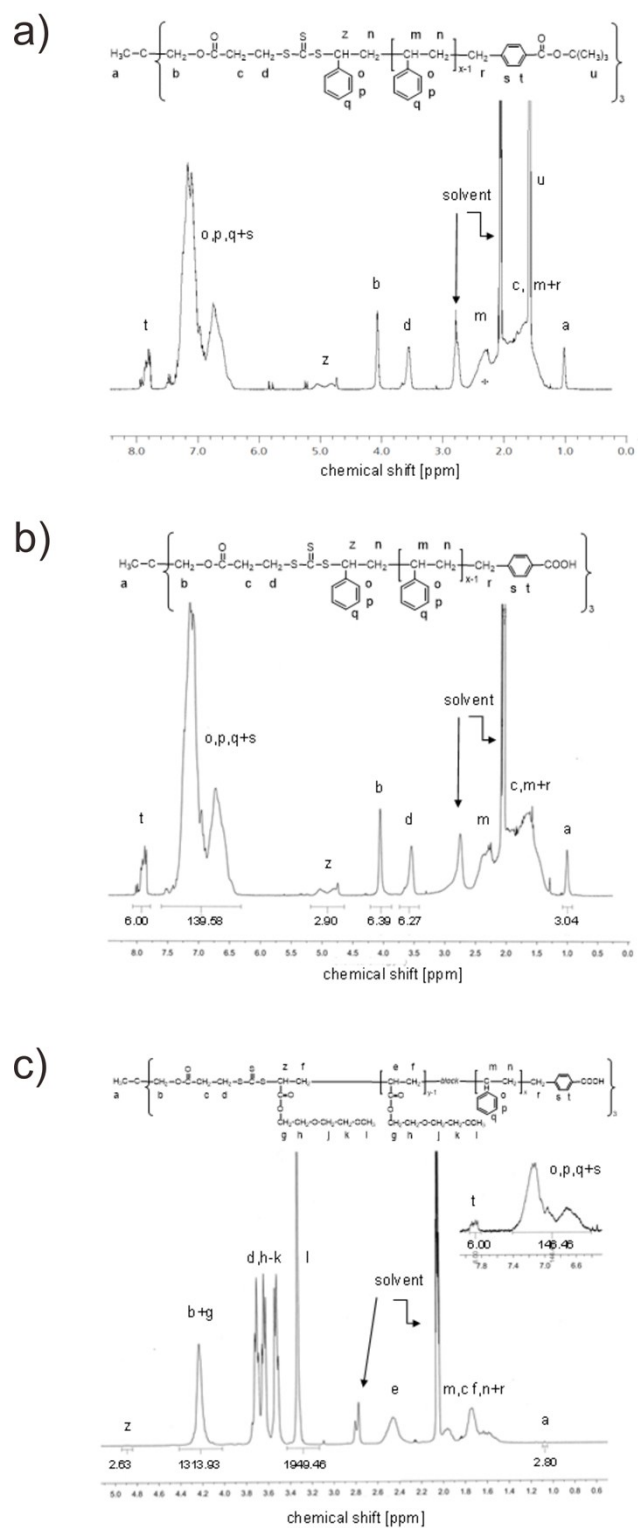


Figure S1. ^1H NMR spectra (a) of star polymer precursor $(\text{PS}^*)_3$ with t-butyl ester end groups, (b) of star polymer precursor $(\text{PS})_3$ after removal of the t-butyl ester end groups, and (c) of star block copolymer $(\text{PMDEGA-}b\text{-PS})_3$.

End-group functionality is estimated by comparing the integral of the signal at 8.0 ppm (characteristic for the reinitiating R-group) with the integral of the signal "a" at ca.1.1 ppm (characteristic for the -CH₃ moiety of the Z-group), yielding Z/R = 1. The quantification of the Z/R-group ratio was cross-checked by the integrals of other discernable signal groups characteristic for the Z-group (signals "b", "d", and "z"), which provided the same value within the precision of the analysis.

The number average molar mass M_n of the star block copolymer (PMDEGA-*b*-PS)₃ is determined combining equation S1 and S3

$$DP_n^{arm} = integral(l)/3 \quad (S3)$$

after normalization of the integrals to an intensity value equivalent of 6 protons for signal "t", and assuming that the molar mass M_n , and thus also DP_n^{arm} , of the star macroRAFT agent (PS)₃ is preserved during the chain extension polymerization.

With $M_r(CTA)=3800$, $M_r(MDEGA)=174.19$ and $f=3$, we obtain for the polystyrene star block (PMDEGA-*b*-PS)₃ a value of $M_n^{NMR}=117,000$.

This value is corroborated by comparing the integral of the signal group "o, p, q+s" between 7.5 and 6.2 ppm of the styrene repeat unit to the integral of the signal "l" at 3.3 ppm of the MDEGA repeat unit, yielding within the precision of the analysis the same value.

Moreover, end-group functionality is estimated by comparing the integral of the signal at 8.0 ppm (characteristic for the reinitiating R-group) with the integral of the signal "a" at ca.1.1 ppm (characteristic for the -CH₃ moiety of the Z-group), yielding a ratio Z/R = 0.93. This suggests that majority of the star polymers bear 3 arms. The quantification of the Z/R-group ratio was cross-checked by the integral of other

discernable signal groups characteristic for the Z-group (signal "z"), which provided the same value within the precision of the analysis.

Characterization of the polymers by size-exclusion chromatography (SEC)

Size-exclusion chromatography (SEC) of the polystyrene star polymer was run with eluent THF at 20 °C using a Waters 515 HPLC isocratic pump equipped with a Waters 2414 Refractive Index detector, a Waters 2487 UV detector and a set of Styragel columns (Waters, HR 5, HR 45, HR 3, 500-100,000 Da). SEC of the star block copolymer was run with eluent DMF containing 1.0 mg mL⁻¹ of LiBr using a Spectra Physics Instruments apparatus equipped with a UV-detector SEC-3010 and a refractive index detector SEC 3010 (WGE-Dr. Bures, Dallgow-Döberitz/Germany), with columns Guard (7.5 x 75 mm) and PolarGel-M (7.5 x 300 mm). All elugrams were calibrated with narrowly distributed linear polystyrene standards (PSS Polymer Standard Service, Mainz/Germany). The elugrams are displayed in Figure S2.

Theoretically expected molar masses M_n^{theo} were calculated *via* equation S4, from the molar ratios monomer to RAFT agent, the molar mass of the CTA, and the gravimetrically obtained yields assuming that they correspond to monomer conversions.

$$M_n^{theo} = conversion \times \left\{ M_r(monomer) \times [monomer] / [CTA] \right\} + M_r(CTA)$$

(S4)

with [monomer] and [CTA] being the molar concentrations of the monomer and the CTA, respectively.

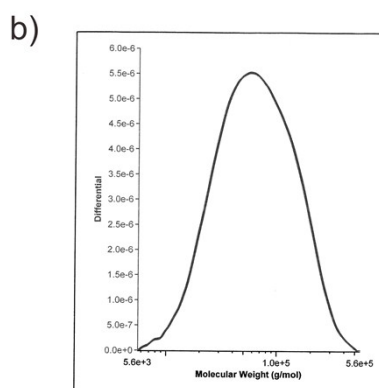
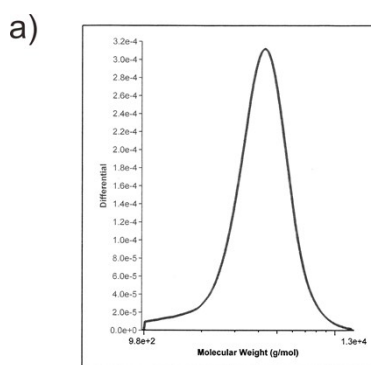


Figure S2. With polystyrene standards calibrated SEC elugrams of (a) of star polymer precursor $(PS^*)_3$ bearing t-butyl ester end groups (eluent THF), and (b) of star block copolymer $(PMDEGA-b-PS)_3$. elugrams (eluent DMF).

Equation used to fit the NR data

As described in the paper from Andrew Nelson,² the NR profile was calculated by the Abeles matrix method.³ It presents identical results to the Parratt recursion relationship⁴ for specular reflection from a stratified medium.

According to this description, the interfaces can be divided into n layers. As the refraction of incident neutron beam can occur in each layer, the value of the wavevector, k , in layer n , can be obtained from equation S5.

$$K_n = [K_0^2 - 4\pi(\rho_n - \rho_0)]^2 \quad (\text{S5})$$

in which $K_0 = q/2$

The Fresnel reflection coefficient between layer n and layer $n+1$ can be calculated from equation S6.

$$r_{n,n+1} = \frac{K_n - K_{n+1}}{K_n + K_{n+1}} \quad (\text{S6})$$

Because the interface between each layer is impossible to be perfectly smooth, the roughness/diffuseness of each interface modifies the Fresnel coefficient and is accounted for an error function equation S7.⁵

$$r_{n,n+1} = \frac{K_n - K_{n+1}}{K_n + K_{n+1}} \exp(-2k_n k_{n+1} \sigma_{n,n+1}^2) \quad (\text{S7})$$

In addition, a phase factor β (equation S8) is introduced to account for the thickness (d_n) of each layer:

$$\beta_n = k_n d_n \quad (\text{S8})$$

To calculate each layer, a characteristic matrix C_n (equation S9) is applied:

$$C_n = \begin{bmatrix} \exp\beta_n & r_n \exp(\beta_n) \\ r_n \exp(-\beta_n) & \exp(-\beta_n) \end{bmatrix} \quad (\text{S9})$$

The obtained matrix (equation S10) is defined as the product of these characteristic matrices,

$$M = \prod_{n=0}^n C_n \quad (\text{S10})$$

And the reflectivity can be calculated by equation S11:

$$R = \left| \frac{M_{11}}{M_{12}} \right|^2 \quad (\text{S11})$$

A minimum of five variables are required to fit each reflectivity data curve: (1) the instrumental scale factor. It is used if the reflectivity below the critical angle is not equal to 1. (2) The SLD values of the super-phases. (3) The SLD value of the sub-phase. These two values can be obtained from the literature. (4) The sample backgrounds. A constant value is added at all q values and represents q -independent incoherent scattering and instrument backgrounds. (5) The Gaussian roughness of the substrate, which is used to describe the substrate roughness.

Additionally, four values are required for each layer: (1) the layer thickness (d), (2) material scattering length density (ρ), (3) solvent penetration ($\%solv$) and (4) layer roughness (σ).

GISAXS data modeling

Horizontal line cuts were modeled in the framework of the distorted wave Born approximation (DWBA) to obtain information about lateral structures using the so-called effective interface approximation.⁶⁻⁸ The differential cross-section as a function of solid angle is described in equation S12:

$$\frac{d\sigma}{d\Omega} = \frac{A\pi^2}{\lambda^4} (1 - n^2)^2 |T_i|^2 |T_f|^2 P_{diff}(\vec{q}) \propto P_{diff}(\vec{q}) \quad (\text{S12})$$

in which A is the size of surface illuminated by the X-ray beam, λ is the wavelength applied, n is the refractive index, T_i and T_f are the Fresnel transmission functions of the incident and scattered X-ray beams, and $P_{diff}(\vec{q})$ is the factor accounting for the diffuse scattering. Because the incident and exit angles stay unchanged, the Fresnel transmission functions only act as scaling factors during the GISAXS measurements. Therefore, the intensity is proportional to the diffuse scattering factor $P_{diff}(\vec{q})$. In the case of N identical objects positioned in a geometrical arrangement, the diffuse scattering factor can be determined by equation S13:⁶⁻⁸

$$P_{diff}(\vec{q}) \propto N |F(\vec{q})|^2 S(\vec{q}) \quad (\text{S13})$$

where $F(\vec{q})$ and $S(\vec{q})$ are the form factor and structure factor, respectively. $F(\vec{q})$ is the Fourier transform of the electron density distribution ρ_e . Thus, it depends on the shape and size of the scattering objects, which can be described by equation S14.

$$F(\vec{q}) = \int_V \rho_e(\vec{r}) e^{2\pi i(\vec{q}\vec{r})} dV \quad (\text{S14})$$

The local monodisperse approximation (LMA) and a 1D paracrystal arrangement of the scattering objects are applied. The polydispersity of the scattering objects is

described with a Gaussian distribution function. The scattering objects, which are the PS domains in PMDEGA matrix, are considered to have a sphere shape and are modelled with the form factor as equation S15.

$$F_{sphere}(\vec{q}, R) = \exp[iq_z R] \int_0^{2R} 2\pi R_z^2 \frac{J_1(q_r R)}{q_r R} e^{(-iq_z \frac{H}{2})} dz \quad (S15)$$

in which R is the radius of the sphere. q_r equals to the square root of $(q_x^2 + q_y^2)$ and J_1 is the first order Bessel function. Within the framework of a 1D paracrystal arrangement, a Gaussian distribution σ and a mean domain inter distance D are assumed for the scattering objects. Thus, the spatial arrangement of the scattering objects (structure factor $S(\vec{q})$) is modelled as equation S16.

$$S(\vec{q}) = \frac{1 - e^{(\pi(\sigma q_y D)^2)^2}}{1 + e^{(\pi(\sigma q_y D)^2)^2} - 2e^{(\pi(\sigma q_y D)^2)} \cos(q_y D)} \quad (S16)$$

The diffusion model for the swelling process probed by white light interferometry

The swelling process of the (PMDEGA-*b*-PS)₃ films can be quantitatively described by considering kinetic effects, the humidity-induced kinetics and the intrinsic swelling kinetics of the films.⁹⁻¹¹ The equilibrium absorption of water molecules in (PMDEGA-*b*-PS)₃ films at a certain relative humidity P/P_{sat} can be described by the regular solution theory (equation S17).

$$\ln\left(\frac{P}{P_{sat}}\right) = \ln\left(1 - \frac{d_{ini}}{d_{max}}\right) + \left(1 - \frac{V_{D_2O}}{V_{(PMDEGA-b-PS)_3}}\right) \frac{d_{ini}}{d_{max}} + \chi \left(\frac{d_{ini}}{d_{max}}\right)^2 \quad (S17)$$

in which V_{D_2O} and $V_{(PMDEGA-b-PS)_3}$ are the molar volumes of D₂O and (PMDEGA-*b*-PS)₃, respectively. χ is the Flory-Huggins parameter between D₂O and (PMDEGA-*b*-PS)₃. d_{ini} and d_{max} are the initial and maximum swollen thickness of (PMDEGA-*b*-PS)₃ films, respectively. From equation S17, the maximum swelling ratio d_{max}/d_{ini} as a function of the time-dependent relative humidity (P/P_{sat}) and the Flory-Huggins parameter (χ) can be obtained.

If the higher order of intrinsic swelling from the (PMDEGA-*b*-PS)₃ films is neglected, the temporal evolution of relative film thickness can be described by equation S18.¹²⁻

14

$$\frac{d}{d_{ini}} = \frac{d_{max}(\chi, t)}{d_{ini}} - \left(\frac{d_{max}(\chi, t)}{d_{ini}} - 1\right) B \exp\left(-\frac{t}{\tau}\right) \quad (S18)$$

where τ is the relaxation time and B is a constant.

Table S1. Parameters obtained from fitting of the film thickness (probed by white light interferometry) as a function of time during the hydration of the as-prepared star shaped (PMDEGA-*b*-PS)₃ film in D₂O vapor atmosphere at 23 °C.

p/p_{sat}	0.95 ± 0.01
d_{max}/d	2.60 ± 0.03
B	0.97 ± 0.01
χ	0.45 ± 0.01
τ (s)	332 ± 5

Equations used for description of diffusion process

The dynamic hydration process of (PMDEGA-*b*-PS)₃ films can be described by a diffusion process with a model explaining gel swelling kinetics.¹⁵ Based on this model, the swelling or the shrinking process is assumed to be not a pure diffusion process, but rather follow the first-order kinetics. According to this assumption, the shear modulus (M_{shear}) is related to the net osmotic modulus (M_{os}) and the osmotic bulk modulus (K_{bulk}).¹⁴ Their relationship is presented in equation S19:

$$R = \frac{M_{shear}}{M_{os}} = \frac{M_{shear}}{K_{bulk} + \frac{4}{3}M_{shear}} \quad (S19)$$

While the swelling or shrinking processes are described by equation S20:

$$\frac{\varphi_{D_2O}^{(\infty)} - \varphi_{D_2O}}{\varphi_{D_2O}^{(\infty)}} = \sum_{n=1}^{\infty} B_n \exp\left(-\frac{t}{\tau_n}\right) \quad (S20)$$

In which, φ_{D_2O} and $\varphi_{D_2O}^{(\infty)}$ are the D₂O absorbed at time t and infinite time (the equilibrium state of swelling), respectively. B is related to the shear modulus (M_{shear}) and the osmotic modulus (M_{os}), while τ_n is the relaxation time of the n -th mode. If neglecting all high-order terms ($n \geq 2$), the former equation can be rewritten by equation S21.

$$\ln\left(\frac{\varphi_{D_2O}^{(\infty)} - \varphi_{D_2O}}{\varphi_{D_2O}^{(\infty)}}\right) = \ln B_1 - \frac{t}{\tau_1} \quad (S21)$$

In which B_1 is related to R by equation S22.

$$B_1 = \frac{2(3 - 4R)}{\alpha_1^2 - (4R - 1)(3 - 4R)} \quad (S22)$$

The relaxation time τ_1 is related to the diffusion coefficient D_c from equation S23:

$$D_c = \frac{3Z_\infty^2}{\tau_1 \alpha_1^2} \quad (\text{S23})$$

α_1 is a function of R , described in equation S24:

$$R = \frac{1}{4} \left[1 + \frac{\alpha_1 J_0(\alpha_1)}{J_1(\alpha_1)} \right] \quad (\text{S24})$$

Z_∞ is the swollen thickness in the final equilibrium state. J_0 and J_1 are the 0th and 1st order of Bessel functions. By calculation of $(\varphi_{D_2 \rho}^{(\infty)} - \varphi_{D_2 \rho}) / \varphi_{D_2 \rho}^{(\infty)}$, B_1 and τ_1 can be first obtained. Afterwards R and D_c can be obtained as well.

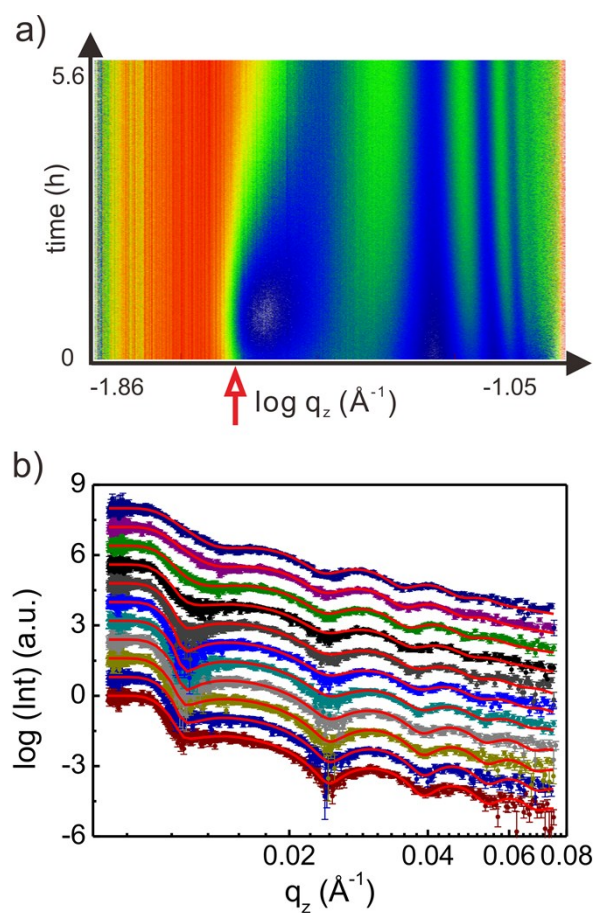


Figure S3. Hydration of the as-prepared star-shaped (PMDEGA-*b*-PS)₃ film in D₂O vapor atmosphere at 23 °C: (a) Two-dimensional intensity presentation (mapping) of the NR data as a function of hydration time with a logarithmic q_z axis. The red arrow marks the initial position of the critical angle. Different scattering intensities are displayed with different color (bright and dark mean high and low intensity, respectively). (b) NR curves (dots) shown together with the model fits (red lines) measured at 10, 310, 610, 1610, 2610, 3710, 4910, 7410, 11410, 17410 and 20210 s. The curves are shifted vertically for clarity of the presentation.

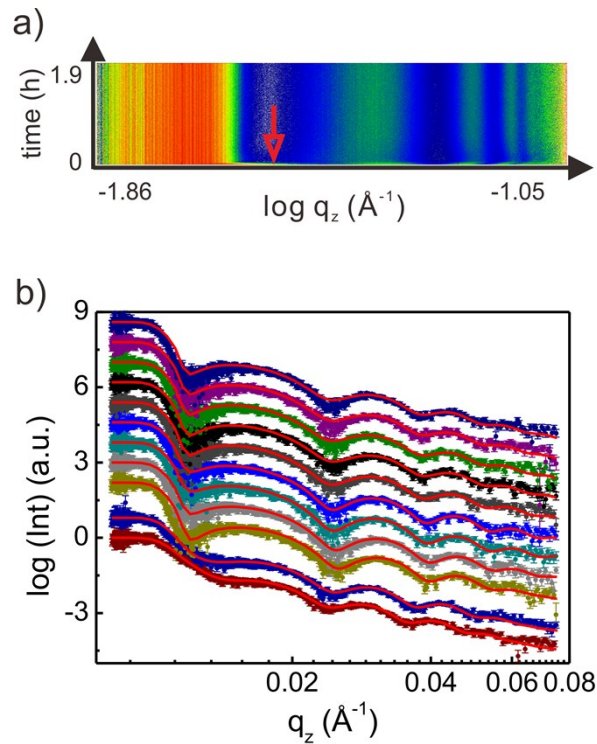


Figure S4. Response of the swollen star-shaped (PMDEGA-*b*-PS)₃ film in D₂O vapor atmosphere after the temperature rapidly increased from 23 °C to 35 °C: (a) Two-dimensional intensity presentation (mapping) of the neutron reflectivity data as a function of time with a logarithmic q_z axis. Time 0 means the point after temperature rapidly increases. The red arrow marks the initial position of the critical angle. Different scattering intensities are displayed with different color (bright and dark mean high and low intensity, respectively). (b) Eleven selected NR curves (black dots) shown together with model fits (red lines) measured at 10, 110, 210, 310, 410, 610, 1760, 3760, 4760, 5760 and 6760 s. The curves are shifted vertically for clarity of the presentation.

Table S2.

Parameters obtained from fitting of $\phi(D_2O)$ in the film (probed by neutron reflectivity) as a function of time when the swollen (PMDEGA-*b*-PS)₃ films under thermal stimuli (23 °C→35 °C, 23 °C→45 °C and 23 °C→50 °C) in D₂O vapor atmosphere.

Collapse region:

thermal stimuli	parameters	top layer	middle layer	bottom layer	total
23 °C → 35 °C	B	0.89 ± 0.01	0.91 ± 0.01	0.92 ± 0.01	0.9 ± 0.01
	α	1.54 ± 0.01	1.41 ± 0.01	1.33 ± 0.01	1.48 ± 0.01
	τ (s)	170 ± 5	190 ± 5	170 ± 5	190 ± 5
	D _c (m ² /s)	(1.95 ± 0.02) × 10 ⁻¹⁹	(3.1 ± 0.02) × 10 ⁻¹⁸	(3.58 ± 0.02) × 10 ⁻¹⁹	(7.18 ± 0.02) × 10 ⁻¹⁸
23 °C → 45 °C	B	0.93 ± 0.01	0.95 ± 0.01	0.93 ± 0.01	0.93 ± 0.01
	α	1.25 ± 0.01	1.07 ± 0.01	1.25 ± 0.01	1.25 ± 0.01
	τ (s)	150 ± 5	160 ± 5	140 ± 5	160 ± 5
	D _c (m ² /s)	(4.32 ± 0.02) × 10 ⁻¹⁹	(7.93 ± 0.02) × 10 ⁻¹⁸	(6.14 ± 0.02) × 10 ⁻¹⁹	(1.48 ± 0.02) × 10 ⁻¹⁷
23 °C → 50 °C	B	0.95 ± 0.01	0.94 ± 0.01	0.93 ± 0.01	0.92 ± 0.01
	α	1.07 ± 0.01	1.17 ± 0.01	1.25 ± 0.01	1.34 ± 0.01
	τ (s)	140 ± 5	150 ± 5	140 ± 5	150 ± 5
	D _c (m ² /s)	(3.79 ± 0.02) × 10 ⁻¹⁹	(7.31 ± 0.02) × 10 ⁻¹⁸	(3.6 ± 0.02) × 10 ⁻¹⁹	(1.16 ± 0.02) × 10 ⁻¹⁷

Reswelling region:

thermal stimuli	parameters	top layer	middle layer	bottom layer	total
23 °C → 35 °C	B	0.76 ± 0.01	0.7 ± 0.01	0.69 ± 0.01	0.72 ± 0.01
	α	2.17 ± 0.01	2.38 ± 0.01	2.41 ± 0.01	2.31 ± 0.01
	τ (s)	1600 ± 5	1970 ± 5	1620 ± 5	1890 ± 5
	D _c (m ² /s)	(0.49 ± 0.02) × 10 ⁻²⁰	(2.51 ± 0.02) × 10 ⁻²⁰	(0.41 ± 0.02) × 10 ⁻²⁰	(8.88 ± 0.02) × 10 ⁻²⁰
23 °C → 45 °C	B	0.59 ± 0.01	0.58 ± 0.01	0.57 ± 0.01	0.58 ± 0.01
	α	2.69 ± 0.01	2.71 ± 0.01	2.74 ± 0.01	2.71 ± 0.01
	τ (s)	5350 ± 5	5400 ± 5	5200 ± 5	5300 ± 5
	D _c (m ² /s)	(0.60 ± 0.02) × 10 ⁻²¹	(5.95 ± 0.02) × 10 ⁻²¹	(0.71 ± 0.02) × 10 ⁻²¹	(1.74 ± 0.02) × 10 ⁻²⁰
23 °C → 50 °C	B	0.6 ± 0.01	0.59 ± 0.01	0.58 ± 0.01	0.6 ± 0.01
	α	2.66 ± 0.01	2.69 ± 0.01	2.71 ± 0.01	2.66 ± 0.01
	τ (s)	6300 ± 5	7100 ± 5	5750 ± 5	6000 ± 5
	D _c (m ² /s)	(0.44 ± 0.02) × 10 ⁻²¹	(3.96 ± 0.02) × 10 ⁻²¹	(0.47 ± 0.02) × 10 ⁻²¹	(1.34 ± 0.02) × 10 ⁻²⁰

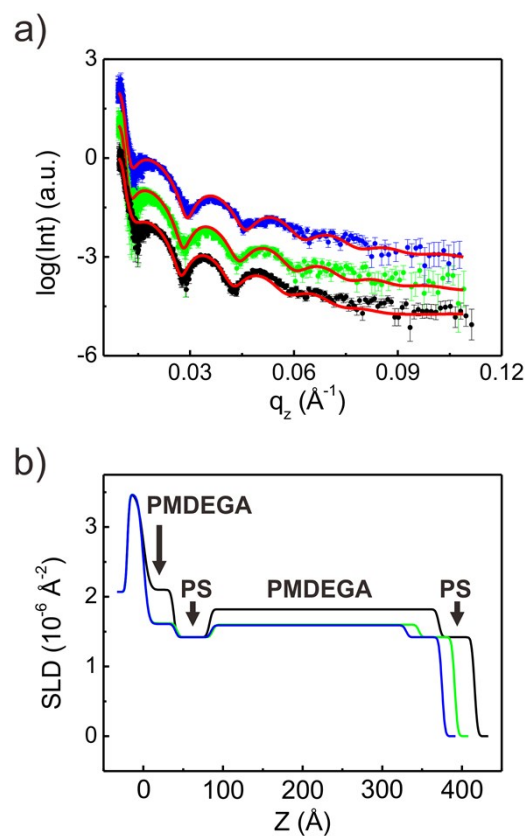


Figure S5. (a) The NR curves of PS-*b*-PMDEGA-*b*-PS films with fitting (red curves) at different final temperatures (black 35 °C, green 45 °C and blue 50 °C). (b) Resulting SLD profiles from the fits of the three NR curves.

References

1. C. Herfurth, P. Malo de Molina, C. Wieland, S. H. Rogers, M. Gradzielski and A. Laschewsky, *Polym. Chem.* 2012, **3**, 1606.
2. A. Nelson, *J. Appl. Crystallogr.* 2006, **39**, 273.
3. O. Heavens, *Optical Properties of Thin Films*. London: Butterworth, 1955.
4. L. G. Parratt, *Phys. Rev.* 1954, **95**, 359.
5. L. Nevot and P. Croce, *Rev. Phys. Appl.* 1980, **15**, 761.
6. P. Müller-Buschbaum: *Structure determination in the thin film geometry using grazing incidence small angle scattering*; in "Polymer Surfaces and Interfaces: Characterization, Modification and Applications", ed. M. Stamm, p.17-46 Springer Berlin (2008).
7. P. Müller-Buschbaum: *A basic introduction to grazing incidence small angle X-ray scattering*; in Special issue of Lecture Notes in Physics on "Applications of Synchrotron Light to Noncrystalline Diffraction in Materials and Life Sciences", Vol. 776, ed. Ezquerra, T.A.; Garcia-Gutierrez, M.; Nogales, A.; Gomez, M.; p.61-90 Springer Berlin (2009).
8. L. Song, W. J. Wang, V. Körstgens, D. M. González, F. C. Löhner, C. J. Schaffer, J. Schlipf, K. Peters, T. Bein, D. Fattakhova-Rohlfing, S. V. Roth and Peter Müller-Buschbaum, *Nano Energy* 2017, **40**, 317.
9. J. Jaczewska, I. Raptis, A. Budkowski, D. Goustouridis, J. Raczowska, M. Sanopoulou, E. Pamuła, A. Bernasik and J. Rysz, *Synth. Met.* 2007, **157**, 726.

10. W. Wang, G. Kaune, J. Perlich, C. M. Papadakis, A. M. Bivigou Koumba, A. Laschewsky, K. Schlage, R. Röhlberger, S. V. Roth, R. Cubitt and P. Müller-Buschbaum, *Macromolecules* 2010, **43**, 2444.
11. D. Magerl, M. Philipp, X. P. Qiu, F. M. Winnik and P. Müller-Buschbaum, Müller-Buschbaum, *Macromolecules* 2015, **48**, 3104.
12. S. Q. Zhou and C. Wu, *Macromolecules* 1996, **29**, 4998.
13. C. Wu and C. Y. Yan, *Macromolecules* 1994, **27**, 4516.
14. Y. Li, and T. Tanaka, *J. Chem. Phys.* 1990, **92**, 1365.
15. W. Wang, E. Metwalli, J. Perlich, C. M. Papadakis, R. Cubitt, and P. Müller-Buschbaum, *Macromolecules* 2009, **42**, 9041.